Bonding Properties of Trinuclear Metal Carbonyls

By **John Evans**, Department of Chemistry, The University, Southampton SO9 5NH

Extended Hückel molecular-orbital calculations have been performed on some trinuclear metal carbonyl species of Fe, Co, and Ni to identify their bonding properties. In addition, formal syntheses of these moieties by the addition of carbonyl ligands to a bare metal triangle and by aggregation of mononuclear carbonyl fragments have been illustrated. Differences between the structural forms and rigidity of complexes containing $Ni_3(CO)_6^{2-}$ or $M_3(CO)_9$ (M = Fe or Co) are rationalised on the basis of the frontier-orbital properties. The nickel compound offers only one cluster fragment orbital of a_2'' symmetry and this contributes to the apparently weak bonding to other groups along the principal axis.

Two stances have recently been adopted for qualitative discussions of the metal–metal bonding in transition-metal carbonyl clusters. One approach centres on the orbital properties of the metal carbonyl fragments which form the cluster vertices.[1] These may be isolobal with a main-group vertex like BH and this is a justification for extending skeletal-electron procedures from main-group to transition elements.[2] An alternative view has been to consider the isolated metal cluster and identify the cluster valence orbitals which are energetically accessible for metal–metal and metal–ligand bonding.[3] This paper follows these two approaches in describing the orbital properties of $Fe_3(CO)_9$, $Co_3(CO)_9$, and $Ni_3(CO)_6$ moieties by a series of extended-Hückel calculations on these species, their constituents, and some adducts.

CALCULATIONS

These were carried out using the program described previously [4] but modified to incorporate the overlap-integral routine in Program 153 of the Quantum Chemistry Program Exchange library. Transition-element valence-orbital ionisation potentials were iterated to charge constituency for mononuclear carbonyl fragments similar to those in the clusters under consideration, *viz.* C_{3v} $Fe(CO)_3$ and $Co(CO)_3$ moieties (C–M–C angle 90°) and a D_{3h} $Ni(CO)_3$ structure.

TABLE 1

Orbital parameters

Element	Orbital	Exponent	H_{ii}/eV
H	1*s*	1.00	−13.60
C	2*s*	1.575	−21.20
	2*p*	1.400	−10.77
O	2*s*	2.200	−32.33
	2*p*	1.975	−15.80
Fe	4*s*	1.37	−10.92
	4*p*	1.37	−5.84
	3*d*	2.722	−11.60
Co	4*s*	1.423	−10.77
	4*p*	1.423	−7.03
	3*d*	2.83	−11.27
Ni	4*s*	1.473	−10.47
	4*p*	1.473	−6.31
	3*d*	2.96	−11.30
As	4*s*	3.037 5	−17.95
	4*p*	1.875	−9.19

Basis sets and structural details used are shown in Tables 1 and 2 respectively. Structural parameters were chosen from crystal-structure data available for $[Fe_3(CO)_9As_2]$,[5] $[Co_3(CO)_9CX]$,[6] $[Co_4(CO)_{12}]$,[7] $[Ni_5(CO)_{12}]^{2-}$,[8] $[Ni_6(CO)_{12}]^{2-}$,[9] $[Mo_2Ni_3(CO)_{16}]^{2-}$,[10] and $[W_2Ni_3(CO)_{16}]^{2-}$.[10] Overlap-matched single-exponent Slater atomic orbitals (STOs) were used for the metal 3*d* functions.[11] A set of valence orbital ionisation potentials (VOIPs) which did not give charge consistency for Fe in $Fe(CO)_3$ (4*s* −12.35, 4*p* −7.37, and 3*d* −13.47 eV) † gave a frontier-orbital pattern qualitatively similar to that shown in Figure 1. Molecular-orbital

TABLE 2

Structural parameters

Compound	Bond lengths/Å		Bond angles/°	
(1) $[Fe_3(CO)_9As_2]$	Fe–Fe	2.68	C–Fe–C	95
	Fe–C	1.80		
	C–O	1.13		
(2) $[Co_3(CO)_9CH]$	Co–Co	2.47	C–Co–C	95
	Co–Co	1.80	Co–Co–C	99
	C–O	1.13		
	Co–C_H	1.92		
	C–H	1.087		
(3) $[Co_3(CO)_6(\mu\text{-}CO)_3(\mu_3\text{-}CO)]^-$	Co–Co	2.47	C–Co–C	108
	Co–C	1.80		
	C–O	1.13		
	Co–C_μ	2.04		
	C–O_μ	1.17		
	Co–C_{μ_3}	1.92		
	C–O_{μ_3}	1.17		
(4) $[Ni_3(CO)_3(\mu\text{-}CO)_3]^{2-}$	Ni–Ni	2.38		
	Ni–C	1.80		
	C–O	1.13		
	Ni–C_μ	1.90		
	C–O_μ	1.17		

stacking and character were similar but the energy scaling differed [$a_1(1)$ −13.72, $e(1)$ −13.71, $e(2)$ −11.18, and $a_1(2)$ −10.16 eV].

RESULTS

Mononuclear Fragments.—Energy-level diagrams for the mononuclear fragments investigated are presented in Figures 1 and 2. As in all the Figures in this paper, these energy levels are immediately above orbitals primarily of CO character which formally contain all the valence electrons of the ligands. The C_{3v} $M(CO)_3$ moieties have been previously studied in detail [1] and the general features of the frontier region were reproduced in this study, *i.e.* three low-lying orbitals, primarily 3*d* in character, and three higher-energy fragment orbitals (1σ and 2π) directed for cluster bonding. The fragment D_{3h} $Ni(CO)_3$ (9) differs in having five occupied low-lying 3*d* orbitals and a lowest-unoccupied molecular orbital (l.u.m.o.) which is of CO π*, nickel $4p_z$ character. The fragment in $Ni_3(CO)_6^{2-}$ (4) is a planar $M(CO)_3$ unit of local C_{2v} symmetry with the two potentially bridging carbonyl groups bent at carbon. This group can be formed

† Throughout this paper = 1 eV ≈ 1.60 × 10^{-11} J.

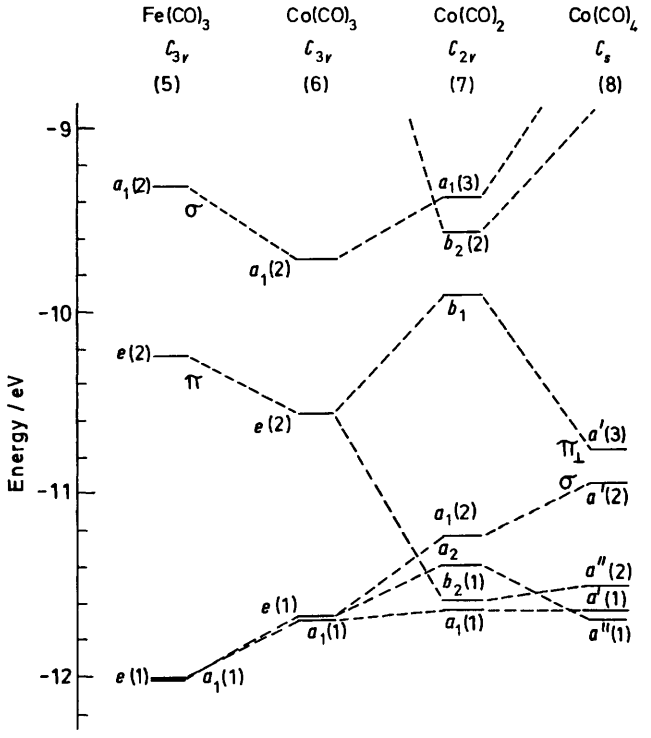

FIGURE 1

from (9) by widening one C–Ni–C angle to 162° (10) and then modifying the two distorted carbonyl groups into a bridging geometry (11). The effects of this procedure on the frontier orbitals are shown in Figure 2. The e' set of (9) are split markedly forming a raised σ fragment orbital ($d_{x^2-y^2}$) $a_1(2)$ in (10). Bending the carbonyl groups to form (11) stabilises

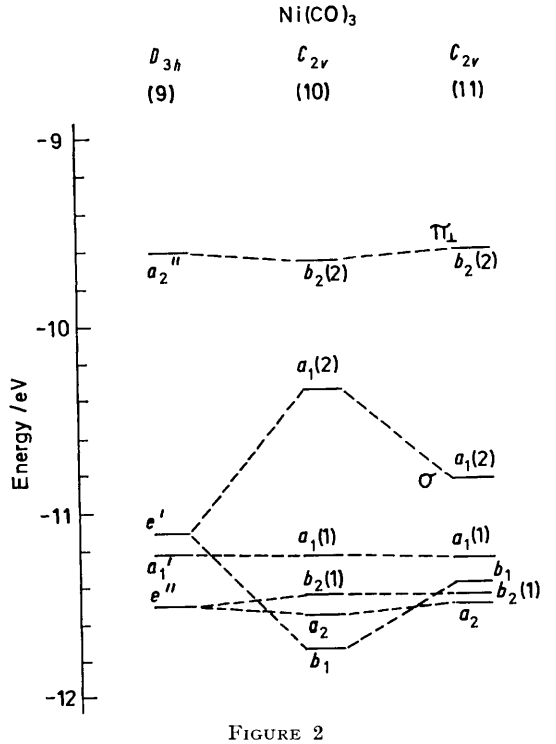

FIGURE 2

this orbital which has good directional properties for cluster bonding. The l.u.m.o. is not markedly altered, becoming the $b_2(2)$ of (11) of $\pi_\perp$ symmetry with respect to a

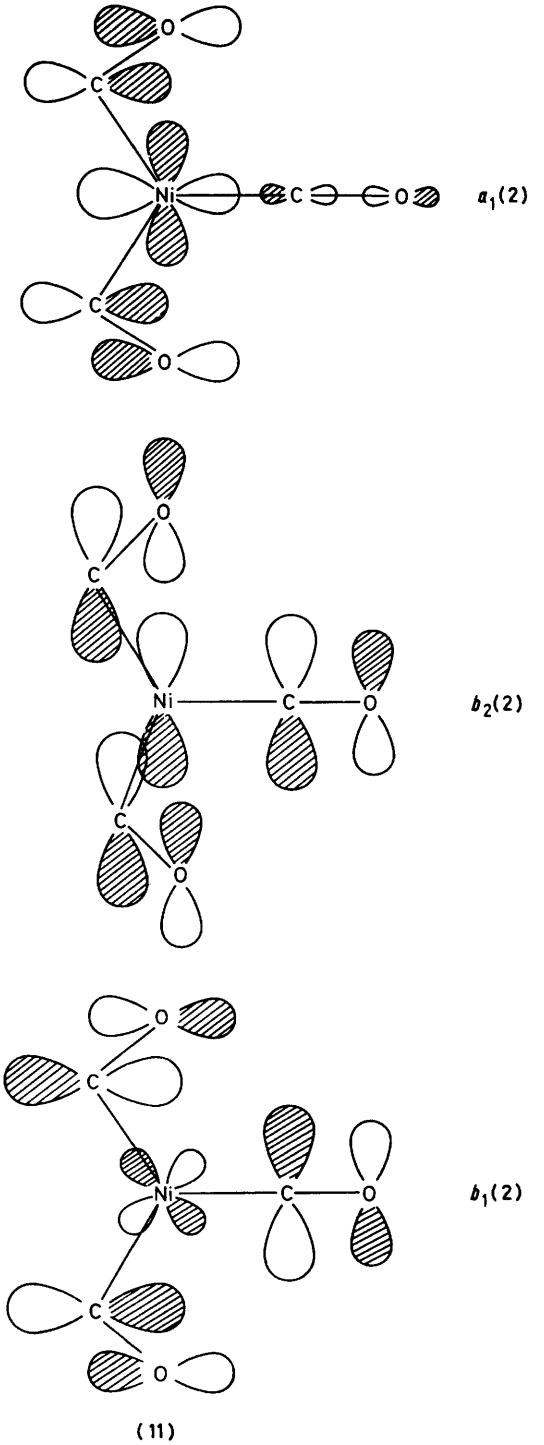

(11)

potential trimer. A $\pi_\parallel$ orbital, $b_1(2)$, is the next highest orbital but at −8.52 eV requires considerable stabilisation before it would attain the 3*d* VOIP.

Fragments of the bridged structure $Co_3(CO)_{10}^-$ (3) were also studied. Thus $Co(CO)_2$ (7) has four low-lying 3*d*

orbitals and three fragment orbitals of σ [$a_1(3)$] and π [$b_1(1)$ and $b_2(2)$] nodal character. Addition of two bridging CO groups to form (8) destabilises the $a_1(3)$ and $b_2(2)$ levels. The $a'(2)$ and $a'(3)$ orbitals form energetically favourable fragment orbitals of σ and π symmetry respectively (with respect to a notional trimer). Again a potential $\pi_{\|}$ fragment, $a''(3)$, is energetically unfavourable (−8.68 eV).

Metal Triangles.—Calculations on three equilateral metal triangles (Fe_3, Co_3, and Ni_3) produced similar patterns. The lowest orbital was of a_1' symmetry and 4*s* character with the fifteen 3*d* orbitals in a range of *ca.* −11.0 to *ca.* −11.7 eV. In each case, the next orbital was an *e'* set of out-pointing 4*s*–4*p* hybrids. The VOIPs used in these particular calculations are appropriate for carbonyl-containing species, rather than bare metal triangles. This procedure was shown to demonstrate the effects of ligand-orbital overlap.

The effects of generating the $Ni_3(CO)_6^{2-}$ anion (4) by first adding three terminal CO ligands and then the three bridges are shown in Figure 3. All correlation lines link predominant parentage rather than representing an energy surface of approach. Although *d*-orbital ordering varied on adding these ligands, the changes were small, reflecting the relatively small overlap integrals involving the *d* orbitals ($|S| \leqslant 0.1$). The $a_1'(1)$ orbital was markedly destabilised as the ligands were added, but there was a counteracting stabilisation of the $4p_z$ π bonding orbital which has a high degree of CO π* character. This maintains the saturation by 32 metal electrons in addition to those of the carbonyl groups.

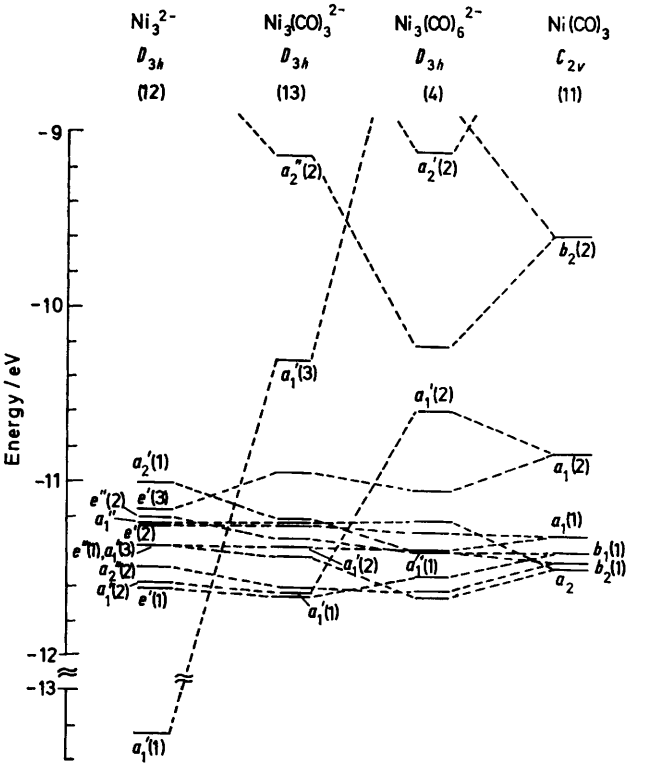

FIGURE 3

The compound $[Fe_3(CO)_9As_2]$ (1) was generated by first adding nine terminal carbonyl groups in a C_{3h} envelope and then adding the two face-bridging As atoms (Figure 4). Again one orbital of the lowest 16 of the bare trimer was destabilised to above *ca.* −10 eV energy (*i.e.* above the 3*d* VOIP). In the non-bridged fragment (15) this formed the $a'(4)$ level at −8.94 eV and is a $\pi_{\|}$* Fe–Fe orbital. In addition, the remaining 15 orbitals split into nine which are low in energy, and six fragment orbitals which are suited for interaction with the six 4*p* atomic orbitals of the two As atoms. The $a'(4)$ orbital of (15) forms the l.u.m.o. of (1) at −8.91 eV.

Both all-terminal (17) and bridged (18) $Co_3(CO)_9$ moieties are known and Figure 5 shows a correlation diagram of each being formed from Co_3. Again, one of 16 metal orbitals was removed from the bonding region. In keeping with the two previous cases, this was a Co–Co $\pi_{\|}$* type orbital in the terminal case [$a_2'(1)$ of (16)] and the Co–Co 4*s* σ orbital in the bridged structure [$a_1'(1)$ of (16)]. In both (17) and (18) three orbitals between *ca.* −10 and *ca.* −11 eV were directed towards the vacant face-bridging site.

Molecular Fragments.—There are two aspects of this approach, *viz.* the formation of trimers from mononuclear fragments and the identification of cluster fragment orbitals. The C_{3v} $M(CO)_3$ moieties present three fragment orbitals of σ[$a_1(2)$] and π[$e(2)$] types and these will generate four cluster bonding orbitals (1σ, $2\pi_{\|}$, and $1\pi_{\perp}$) and five

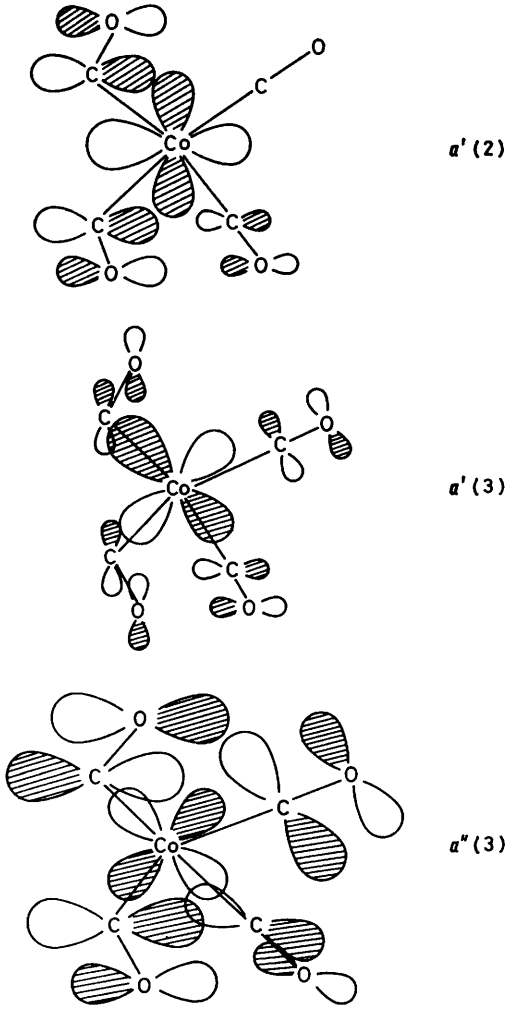

(8)

cluster antibonding orbitals ($2\pi_{\perp}$*, $1\pi_{\parallel}$*, and 1σ*), *cf.* $[B_3H_3]^{n-}$.[4] The fragment orbitals of a $M_3(CO)_9$ cluster would be anticipated to come from this set. A correlation diagram for the construction of $Fe_3(CO)_9$ (15) from $Fe(CO)_3$ (5) and then its interaction with two As atoms is shown in Figure 6. The three in-plane Fe–Fe antibonding orbitals $a'(4)$ and $e'(4)$ of (15) are greatly destabilised, having six orbitals in the cluster frontier region [$e'(3)$ is the highest-occupied molecular orbital (h.o.m.o.) in (5)]. There are three low-lying l.u.m.o.s and these can interact with the $4p$

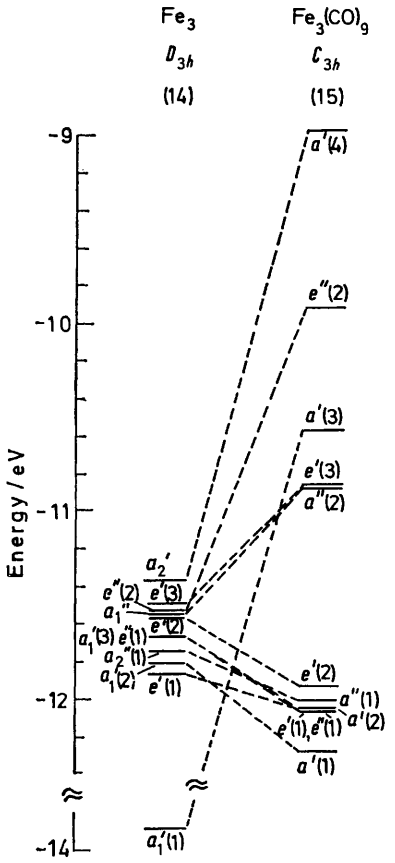

FIGURE 4

orbitals of As to accommodate the extra three ligand electron pairs in (1). Both $a''(2)$ and $a'(3)$ are localised largely on As and the $e''(2)$ set of (15) is most stabilised by interaction with As. The energy-level diagram indicates that the $Fe_3(CO)_9$ moiety is more electronegative than the As $4p$ atomic orbitals and accordingly the charges on Fe and As were computed to be $+0.08$ and $+0.86$ respectively. Neither (1) nor (15) has a significant Fe–Fe reduced overlap population [0.35 for $^3Fe_3$ (14)] and the cage in (1) appears to be largely held by Fe–As bonding (reduced overlap population, 0.24).

The lobal properties of $Co_3(CO)_9$ (16) are very similar to those of (15) with cluster fragment orbitals $a_1(4)$ and $e(5)$ being derived from σ and $\pi_{\perp}$* combinations of $Co(CO)_3$ fragment orbitals; in $^3Co_3(CO)_9^-$, the $e(5)$ set is half filled (Figure 7). On interaction with a face-bridging methine cation [yielding (2)] the $e(5)$ set is stabilised by combination with the vacant CH^+ carbon $2p$ set. The lower-lying C–H lone pair is stabilized by mixing with cluster a_1 character

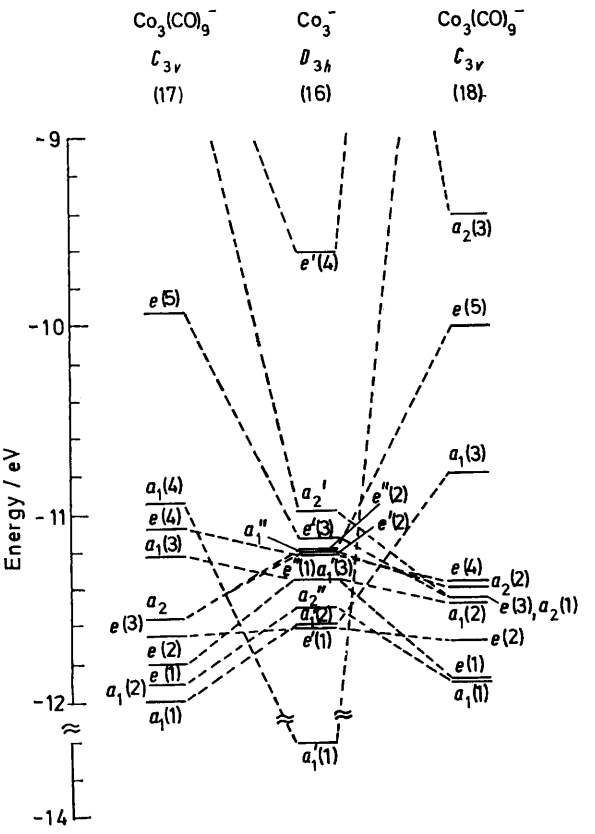

FIGURE 5

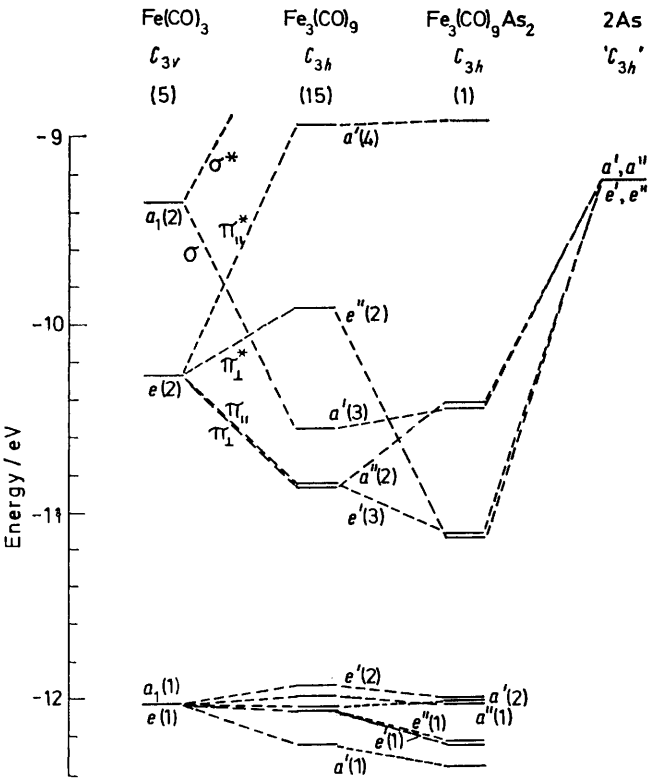

FIGURE 6

and the $a_1(4)$ orbital of (15) becomes antibonding. The two extra skeletal electrons in (2) are accommodated by filling the $e(5)$ set. The Co–Co reduced overlap population in (2) is 0.01, significantly lower than in $^3Co_3(CO)_9^-$ (0.20) and $^3Co_3^-$ (0.42). This parameter suggests that the cage is held primarily by Co–C_H bonding (reduced overlap population, 0.34) and also that the C–H bonds are strengthened by comparison with CH^+ [0.69 in CH^+ and 0.81 in (2)]. A Mulliken population analysis placed a negative charge on the methine carbon in (2) (−0.88) and a positive one on the cobalt atoms (+0.64).

Although the fragment orbitals of the C_s $Co(CO)_4$ moiety (8) have a substantially different energy ordering to C_{3v} $Co(CO)_3$ (6), the electronic properties of the bridged $^3Co_3(CO)_9^-$ isomer (18) are qualitatively similar to those of (17) (Figure 8). The three combinations of the $\pi_{\|}$ fragment,

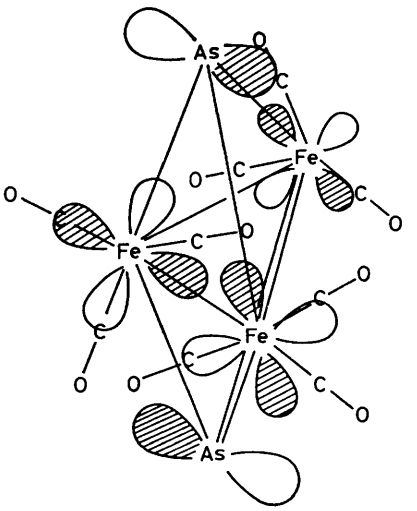

One of $e''(2)$ set of (1)

$a''(3)$ of (8), remain energetically unfavourable although the antibonding combination, greatly stabilised by interaction with the edge-bridging ligands, forms the l.u.m.o. in $Co_3(CO)_{10}^-$ (3). The σ, $\pi_\perp$ distinction is lost due to the removal of the σ_h plane by the carbonyl arrangement and the $a'(2)$ and $a'(3)$ orbitals of (8) yield two sets of cluster fragment orbitals, $a_1(3)$ and $e(5)$, directed at the vacant apical site; the latter set is half filled. Interaction with the face-bridging ligand is qualitatively similar to the previous example, with a cluster a_1 orbital of (18) becoming antibonding and the $e(5)$ set being stabilised to form the h.o.m.o.s of (3). The Co–Co reduced overlap population of (18) at 0.12 is much less than in $^3Co_3^-$, but the metal–metal bonds are supported by the bridging carbon–cobalt interaction (0.29). Both these values are reduced in (3), to −0.01 and 0.22 respectively, but the apical carbon–cobalt interaction (0.18) helps to maintain the heteronuclear cluster. The Mulliken population analysis indicated that 70% of the overall negative charge was localised on the apical CO group.

A comparison between all terminal and bridged isomers of $[Co_3(CO)_9CH]$ and $Co_3(CO)_{10}^-$ was made. In both cases the bridged isomer was favoured but only by 0.2 and 0.5 eV respectively. Essentially these calculations cannot dis-

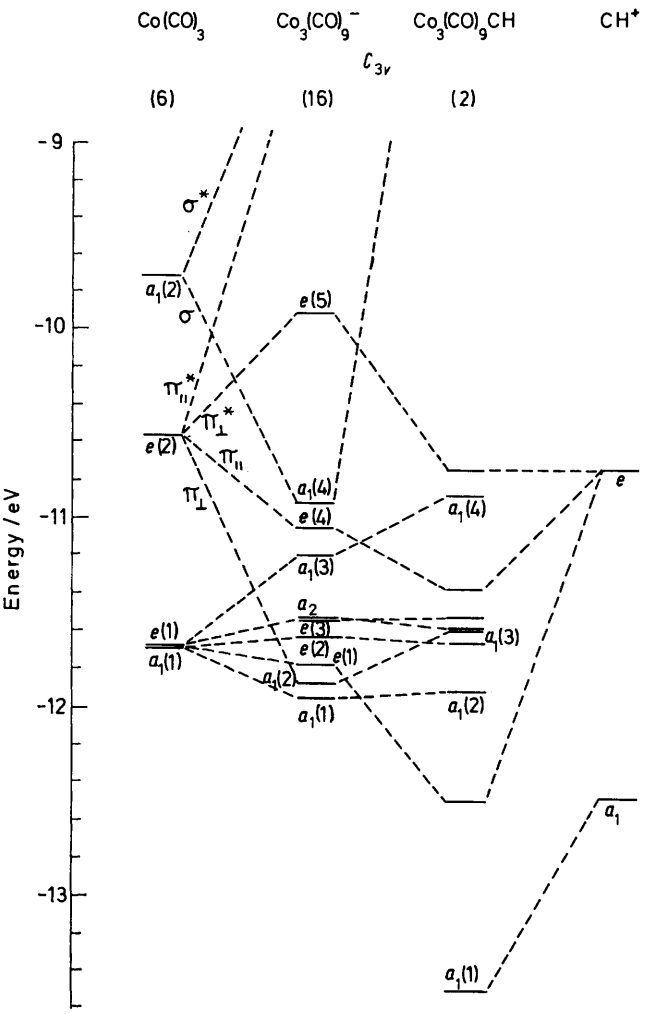

FIGURE 7

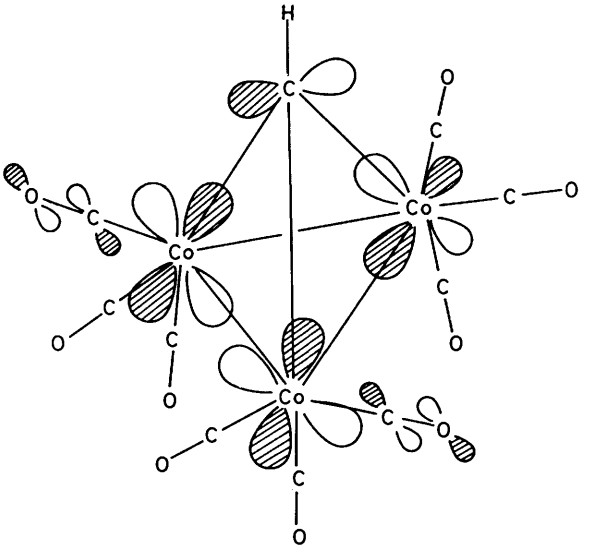

One of $e(5)$ set of (2)

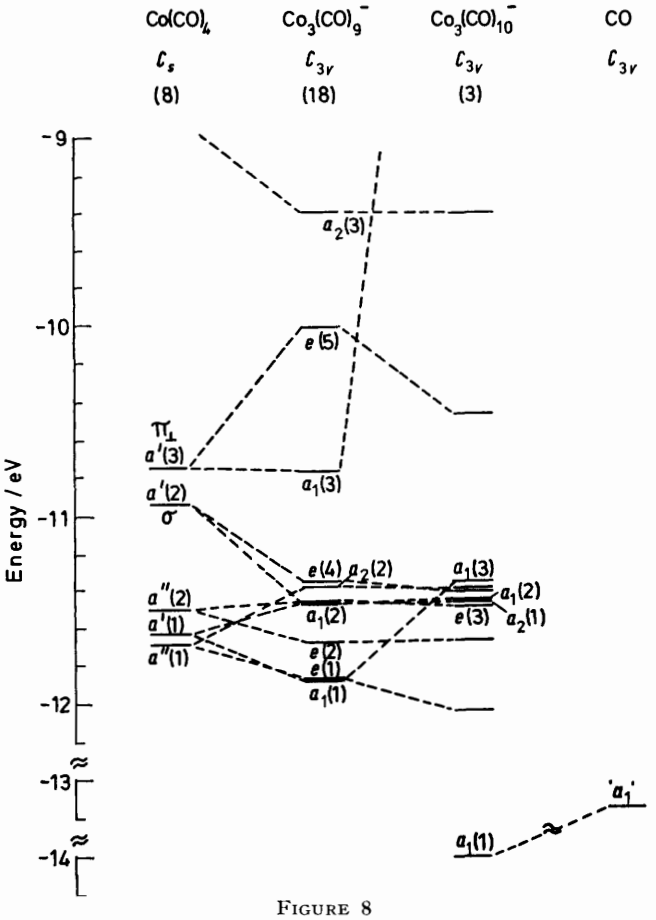

FIGURE 8

criminate between two alternatives, and this is consistent with the coexistence of bridged and non-bridged isomers of some derivatives.[12] In both cases the bridged $Co_3(CO)_9$ moiety was found to be more electron withdrawing.

The $\pi_{\|}$ fragment orbital of the bent $Ni(CO)_3$ unit [$b_1(2)$ of (11)] behaves similarly to that of (8), providing only the l.u.m.o. in $Ni_3(CO)_6^{2-}$ [$a_2'(2)$] (Figure 3). The $\pi_\perp$ fragment orbital of (11) is also above the 3*d* VOIP level and only the bonding combination, $a_2''(2)$, remains in the frontier region forming the anion's h.o.m.o. The σ fragment is now low in energy and all three combinations are occupied. Whereas the $M_3(CO)_9$ moieties each had six accessible cluster fragment orbitals, this planar anion has five. One of these, the $a_2'(2)$, has ϕ symmetry with respect to the C_3 axis and is unlikely to be provided by many capping atoms. Only the h.o.m.o., $a_2''(2)$, has good directional properties perpendicular to the Ni_3 plane and so will probably strongly

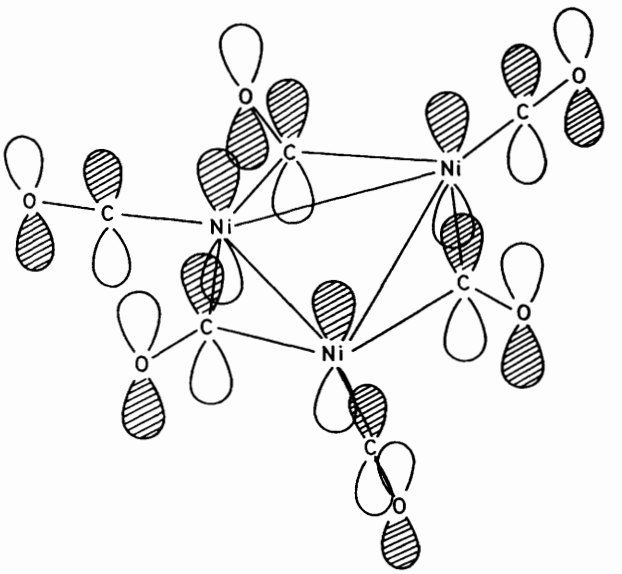

$a_2''(2)$ of (4)

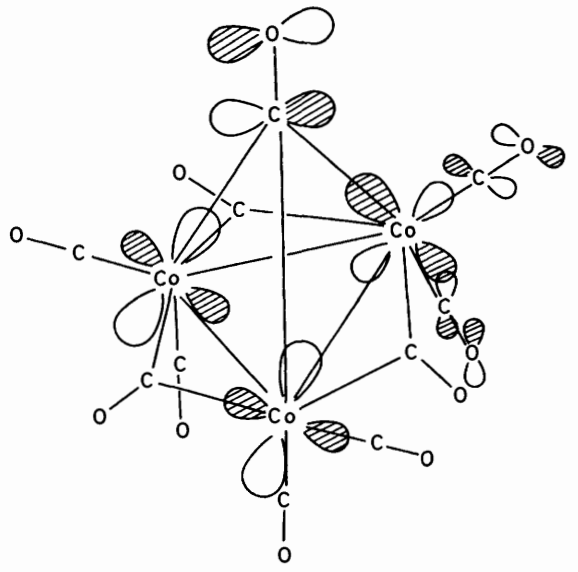

One of e(5) set of (3)

influence interactions in those directions. The reduced overlap populations of Ni–Ni (0.16) and Ni–bridging carbon (0.36) indicate substantial bonding interactions.

DISCUSSION

On electron-counting considerations the three $M_3(CO)_9$ moieties are identical. They each have a set of orbitals primarily of CO character which formally contain electrons from the nine ligands and also have 15 utilisable metal orbitals. The $Ni_3(CO)_6^{2-}$ on the other hand has only six ligands but also has a further 16 occupied orbitals. So while the $M_3(CO)_9$ (M = Fe or Co) species will be saturated with 48 electrons in the metals' valence co-ordination sphere, the nickel system is satisfied with 44. Lauher [3] has traced this difference in electron occupancy to the absence of out-of-plane ligands in (4).

Electron-counting differences are also apparent for species containing these types of cluster fragments. Thus while $[Os_5(CO)_{15}]^{2-}$,[13] containing an equatorial $Os_5(CO)_9$ group, has 72 electrons, both $[Ni_5(CO)_{12}]^{2-}$ (ref. 8) and the $[M_2Ni_3(CO)_{16}]^{2-}$ (M = Cr, Mo, or W) ions [10] are 76-electron species; all these clusters have trigonal-bipyramidal metal cages. However, $[Os_6(CO)_{18}]^{2-}$,[14] $[Ni_6(CO)_{12}]^{2-}$,[9] and $[Pt_6(CO)_{12}]^{2-}$ (ref. 15) are all 86-

electron systems but possess octahedral, trigonal-antiprismatic, and trigonal-prismatic skeletons respectively. These differences can be rationalised by the orbital properties of the $M(CO)_3$ and $M_3(CO)_x$ ($x = 6$ or 9) moieties. The $Fe(CO)_3$ (5) moiety is isolobal with [1] BH and so would be anticipated to generate the same number of skeletal bonding orbitals, *e.g.* six for a trigonal bipyramid and seven for an octahedron. The co-ordination sphere of each iron atom in (5) can be viewed as having 12 electrons in fragment 'core' orbitals below the three fragment 'valence' electrons used in cluster bonding. So a hypothetical $[Fe_5(CO)_{15}]^{x-}$ anion would be anticipated to be a 72-electron species. Alternatively, this ion can be synthesised by capping each face of the $Fe_3(CO)_9$ triangle with an $Fe(CO)_3$ group. Figure 6 shows the compatibility of the six cluster fragment orbitals of $Fe_3(CO)_9$ and those of the capping groups. As in (1) there is a one-to-one correspondence between the six fragment orbitals of the central triangle and the capping atoms.

As demonstrated in Figure 3 and argued above, $Ni_3(CO)_6^{2-}$ is different. Only one orbital, $a_2''(2)$, in the frontier region is suitable for out-of-plane bonding and so 42 of the 44 electrons on the metal atoms may be viewed as core electrons. Sixteen-electron C_{4v} $M(CO)_5$ fragments (M = Cr, Mo, or W) offer a vacant σ-type fragment orbital, and so the apical $M(CO)_5$ units in the $[M_2Ni_3(CO)_{16}]^{2-}$ anions can be considered to be largely held by a multicentred two-electron bond involving the $a_2''(2)$ orbital of (4). This model gives the 76-electron count for these anions. In $[Ni_5(CO)_{12}]^{2-}$ there are two capping 16-electron C_{3v} $Ni(CO)_3$ moieties, each with occupied fragment *e* sets and an empty a_1 fragment orbital (*cf.* Figure 1). The central triangle has only an occupied '*a*' type fragment and again the capping atoms are held with a multicentre two-electron bond; the *e* fragments of the capping $Ni(CO)_3$ moieties have no nearest-neighbour fragment orbitals to interact with. Again a 76-electron count results. Accordingly the weaker axial–equatorial bonds in the metal trigonal bipyramid are reflected in the internuclear distances. In $[Ni_5(CO)_{12}]^{2-}$, the axial–equatorial Ni–Ni separations are 2.81 Å compared with 2.36 Å in the equatorial plane.[6] The mixed-metal pentanuclear anions also form elongated trigonal bipyramids (axial–equatorial distances *ca.* 3.15 Å).

The 86-electron $[Ni_6(CO)_{12}]^{2-}$ anion can be viewed as an $Ni_3(CO)_6$ adduct of $Ni_3(CO)_6^{2-}$, also primarily held by an in-phase combination of the $a_2''(2)$ sets giving a two-electron multicentre bond. Again the interplane metal–metal separation (2.77 Å) is substantially larger than the intraplane internuclear distance (2.38 Å). This approach can also be used to rationalise some properties of the $[\{Pt_3(CO)_6\}_n]^{2-}$ anions.[15] This single σ-type orbital holding the bridged platinum triangles together could allow the observed relative rotation of the triangles in these species ($n = 2$, 3, or 4).[16] If a two-electron bond was primarily responsible for binding these stacked triangles, it would be anticipated that the inter-triangle Pt–Pt distances would increase with cluster size. There is indeed an observed increase, albeit a small one.[15] Finally the weakness of the interplane bonding is supported by the lability of the $Pt_3(CO)_6$ triangles.[16]

These results demonstrate again that the efficiency of skeletal electron-counting schemes depend upon how closely the orbital properties of the molecular fragments coincide with those of the BH groups for which the schemes were developed. They also demonstrate that the fragment approach [1] can be carried over to cluster moieties, and offer an alternative approach to the method of establishing cage-orbital properties from those of the bare metal cluster.[3] Although the two approaches generally coincide, in the latter method care must be taken when considering the geometry of the carbonyl envelope. For clusters of higher nuclearity than three, the effects of distortions of the cluster core or differences in carbonyl geometry may well alter the preferred electron occupancy, as evidenced by the pentanuclear clusters.

I wish to thank the Council of the Royal Society for the award of a Pickering Research Fellowship.

[9/1173 *Received*, 24*th July*, 1979]

REFERENCES

[1] M. Elian and R. Hoffman, *Inorg. Chem.*, 1976, **15**, 1148.
[2] K. Wade, *Adv. Inorg. Chem. Radiochem.*, 1976, **18**, 1.
[3] J. W. Lauher, *J. Amer. Chem. Soc.*, 1978, **100**, 5305.
[4] J. Evans, *J.C.S. Dalton*, 1978, 18.
[5] L. T. J. Delbaere, L. J. Kruczynski, and D. W. McBride, *J.C.S. Dalton*, 1973, 307.
[6] B. R. Penfold and B. H. Robinson, *Accounts Chem. Res.*, 1973, **6**, 73.
[7] C. H. Wei, *Inorg. Chem.*, 1969, **8**, 2384; F. H. Carré, F. A. Cotton, and B. A. Frenz, *ibid.*, 1976, **15**, 380.
[8] G. Longoni, P. Chini, L. D. Lower, and L. F. Dahl, *J. Amer. Chem. Soc.*, 1975, **97**, 5034.
[9] J. C. Calabrese, L. F. Dahl, A. Cavolieri, P. Chini, G. Longoni, and S. Martinengo, *J. Amer. Chem. Soc.*, 1974, **96**, 2616.
[10] J. K. Ruff, R. P. White, jun., and L. F. Dahl, *J. Amer. Chem. Soc.*, 1971, **93**, 2159.
[11] M. Zerner and M. Gouterman, *Theor. Chim. Acta*, 1968, **4**, 44.
[12] T. W. Matheson, B. H. Robinson, and W. S. Tham, *J. Chem. Soc.* (*A*), 1971, 1456.
[13] C. R. Eady, J. J. Guy, B. F. G. Johnson, J. Lewis, M. C. Malatesta, and G. M. Sheldrick, *J.C.S. Chem. Comm.*, 1976, 807.
[14] C. R. Eady, B. F. G. Johnson, and J. Lewis, *J.C.S. Chem. Comm.*, 1976, 302.
[15] J. C. Calabrese, L. F. Dahl, P. Chini, G. Longoni, and S. Martinengo, *J. Amer. Chem. Soc.*, 1974, **96**, 2616.
[16] C. Brown, B. T. Heaton, P. Chini, A. Fumagalli, and G. Longoni, *J.C.S. Chem. Comm.*, 1977, 309.